Articles

Overexpression and Structural Study of the Cathelicidin Motif of the Protegrin-3 Precursor†

Jean Frédéric Sanchez,‡ Franck Wojcik,‡ Yin-Shan Yang,‡ Marie-Paule Strub,‡ Jean Marc Strub,§ Alain Van Dorsselaer,§ Marianne Martin,|| Robert Lehrer,⊥ Tomas Ganz,⊥ Alain Chavanieu,‡ Bernard Calas,‡ and André Aumelas*,‡

Centre de Biochimie Structurale, UMR 5048 CNRS-UM1/UMR 554 INSERM-UM1, Université Montpellier 1, Faculté de Pharmacie, 15 avenue Charles Flahault, 34093 Montpellier Cedex 5, France, Laboratoire de Spectrométrie de Masse Bio-Organique, ECPM, 25, rue Becquerel, 67087, Strasbourg Cedex 2, France, Université Montpellier II, CNRS UMR 5539, CC 107, 34095 Montpellier Cedex 05, France, and Department of Medicine, Center for the Health Sciences, Los Angeles, California 90095

Received May 7, 2001; Revised Manuscript Received September 26, 2001

ABSTRACT: Numerous precursors of antibacterial peptides with unrelated sequences share a similar prosequence of 96−101 residues, referred to as the cathelicidin motif. The structure of this widespread motif has not yet been reported. The cathelicidin motif of protegrin-3 (ProS) was overexpressed in *Escherichia coli* as a His-tagged protein to facilitate its purification. The His tag was then removed by thrombin cleavage. In addition, the complete proprotegrin-3 (ProS-PG-3) (120 residues) was overexpressed in baculovirus-infected insect cells. As it contained the antibacterial peptide protegrin-3 in its C-terminal part, ProS-PG-3 contained four disulfide bonds. At neutral pH, ProS and ProS-PG-3 adopted two slowly exchanging conformations that existed in a ratio of 55/45. This ratio was progressively modified at acidic pH to reach a 90/10 value at pH 3.0, suggesting that electrostatic interactions are involved in such a conformational change. Therefore, the structural study of the main conformer was undertaken at pH 3.0 by circular dichroism, mass spectrometry, and homo- and heteronuclear NMR. In parallel, a model for the ProS structure was built from the X-ray structure of the chicken cystatin. ProS and the chicken cystatin share two conserved disulfide bonds as well as a high conservation of hydrophobic residues. The ProS model features the conservation of a hydrophobic core made of the interface between the N-terminal helix and the wrapping β-sheet. Although the full assignment of the main conformer of ProS could not be obtained, available NMR data validated the presence of the N-terminal helix and of a four-stranded β-sheet, in agreement with the cystatin fold. Moreover, we clearly demonstrated that ProS and ProS-PG-3 share the same global structure, suggesting that the presence of the highly constrained β-hairpin of protegrin does not significantly modify the structure of the cathelicidin motif of the protegrin precursor.

Protegrins (PG-1 to PG-5, 16−18 residues) are a family of antibacterial peptides isolated from porcine leucocytes (*1*). They form an arginine-rich β-sheet stabilized by two disulfide bridges and amidated at the C-terminus (*2*, *3*). Protegrins are initially synthesized as precursors of 149 residues (147 residues for PG-2) with three regions: a signal peptide (sequence 1−29), a prosequence (sequence 30−130 referred to as ProS), and the PG-1 sequence (sequence 131−148). The Gly^{149} is removed in a conventional amidation step (*4*−*6*). It has been shown that PG[1] has no antibacterial activity when bound to its prosequence and that the cleavage of the $V^{130}-R^{131}$ amide bond by an elastase-like enzyme yielded the active protegrin (*7*, *8*). A similar inactivating role has been reported for the prosequence of the human α-defensin HNP-1 (*9*) and other antimicrobial peptides. It has been proposed that intramolecular inactivation depends on electrostatic interactions between the antibacterial peptide, usually positively charged, and the negatively charged groups of the prosequence (*9*).

Interestingly, precursors of numerous antibacterial peptides of unrelated sequences and three-dimensional structures have prosequences which share a high degree of similarity (*10*−*17*). ProS belongs to this family of prosequences, the cathelicidin family, which currently contains 28 sequences.

† This research was supported by a grant from the Ministère de l'Education Nationale, de la Recherche, et de la Technologie (J.F.S.).

* To whom correspondence should be addressed. Tel: 33 467 043 432. Fax: 33 467 529 623. E-mail: aumelas@cbs.univ-montp1.fr.

‡ Centre de Biochimie Structurale.

§ Laboratoire de Spectrométrie de Masse Bio-Organique.

|| Université Montpellier II.

⊥ Center for the Health Sciences.

[1] Abbreviations: CD, circular dichroism; 1D, 2D, and 3D, one, two, and three dimensional; DQF-COSY, double-quantum-filtered correlation spectroscopy; DTT, 1,4-dithiothreitol; ES-MS, electrospray mass spectrometry; HSQC, heteronuclear single-quantum coherence; IPTG, isopropyl β-D-thiogalactopyranoside; NMR, nuclear magnetic resonance; NOE, nuclear Overhauser effect; NOESY, nuclear Overhauser effect spectroscopy; PG, protegrin; ProS, prosequence of the protegrin; ProS-PG-3, proprotegrin-3; RP-HPLC, reverse-phase high-performance liquid chromatography; SDS−PAGE, sodium dodecyl sulfate−polyacrylamide gel electrophoresis; TOCSY, total correlation spectroscopy; TPPI, time-proportional phase incrementation; TSP-d_4, sodium 2,2,3,3-tetradeuterio-3-(trimethylsilyl)propionate; WATERGATE, water suppression by gradient-tailored excitation.

10.1021/bi010930a CCC: $22.00
Published on Web 12/07/2001

In turn, the cathelicidin sequence falls within the cystatin superfamily, which also includes cystatin, kininogen, and stefin proteins (*12*, *18*). According to their molecular weight and the presence or absence of disulfide bonds, these proteins belong to three different classes. Among these proteins which contain two characteristic disulfide bonds, the structures of the highly homologous chicken and quail cystatins were determined (*19*−*22*), and recently, it has also been shown that the human cystatin C refolds to produce a very tight 2-fold symmetry dimer which retains the secondary structure of the monomeric form (PDB entry 1G96) (*23*). The structures of two animal cystatins lacking disulfide bonds, cystatin A (or stefin A) (PDB entries 1DVC and 1DVD) (*24*) and cystatin B (or stefin B) (PDB entry 1STF) (*25*), were also reported. All of these structures, including the monomer-like of the human cystatin C, display a similar global fold, which consists of an N-terminal helix cradled by a β-sheet consisting of four to five antiparallel β-strands. Two plant proteins devoid of disulfide bonds were also found to adopt a similar fold, monellin, a sweet-tasting protein (PDB entry 1MNL) (*26*) and oryzacystatin-I, a cysteine proteinase inhibitor of rice, *Oryza sativa* L. japonica (PDB entry 1EQK) (*27*).

The bovine cathelicidin contains two disulfide bonds in the 1−2, 3−4 arrangement (*12*). Such an arrangement would correspond to C^{85}−C^{96} and C^{107}−C^{124} disulfide bonds for ProS (see Discussion). A CD study of probactenecin, which contains this motif, showed a content of about 50% of extended conformation and less than 20% of α-helical conformation. Moreover, these authors showed that the helix was mainly located in the proregion of the probactenecin. However, the detailed three-dimensional structure of this widespread cathelicidin motif is not yet known. To characterize the cathelicidin structure and the hypothetical interactions (electrostatic or/and hydrophobic) between the antibacterial peptide and the prosequence, we overexpressed ProS and the proprotegrin-3 (referred to as ProS-PG-3), the latter consisting of ProS extended at its C-terminus by the protegrin-3 sequence. We describe here a model for ProS based on the structure of the chicken cystatin and the structural studies of ProS overexpressed in *Escherichia coli*. On the basis of NMR data, we observed that the ProS structure adopts two pH-dependent conformations in slow exchange on the proton chemical shift time scale. Moreover, an N-terminal helix and a four-stranded β-sheet, consistent with the model, were identified in the ProS structure. Finally, NMR data of ProS are compared with those of ProS-PG-3 overexpressed in the baculovirus system.

MATERIALS AND METHODS

Chemicals. Bovine thrombin was from Calbiochem. Culture media were from Gibco BRL (Cergy Pontoise, France). Primers for PCR amplification were from Eurogentec.

Overexpression of ProS in pET-15b. A PCR product containing the coding sequence of ProS (30−130) was generated from a pBluescript plasmid containing the preproprotegrin-3 cDNA (*8*). The amplified cDNA was subcloned into the *Nde*I/*Bam*HI sites of the pET-15b plasmid vector (Novagen) leading to the N-terminus in frame fusion with the His tag. *E. coli* BL21(DE3) transformed with the recombinant plasmid was used to inoculate 400 mL of medium (20 g/L tryptone, 10 g/L yeast extract, 5 g/L sodium citrate, 5 g/L KH_2PO_4, adjusted to pH 7.0) containing 100 μg/mL ampicillin. After overnight growth at 37 °C, the culture was used to inoculate 4 L of the same medium supplemented with ampicillin (100 μg/mL), $MgSO_4$ (10 mM), glucose (5 g/L), biotin (1 mg/L), thiamin (10 mg/L), and nicotinamide (10 mg/L) and grown at 37 °C for 3 h. Expression was induced for 3 h by the addition of 1 mM IPTG. The cells were harvested by centrifugation and stored at −80 °C.

Purification of the His-Tagged ProS. Cells, 20 g wet weight, were thawed and resuspended in 50 mL of ice-cold buffer A (100 mM Tris-HCl, pH 7.5, 150 mM NaCl) containing 5 mM benzamidine. The mixture was homogenized and frozen/thawed three times. The lysate was kept on ice and probe sonicated for 1 min with 0.1 s bursts at 340 W. The particular material was then removed by centrifugation at 20000*g* for 15 min at 4 °C. The supernatant was further clarified by centrifugation at 90000*g* for 40 min. The supernatant (44 mL) was applied onto a Q-Sepharose (Amersham Pharmacia Biotech) column (20 × 2.6 cm) equilibrated with buffer A. The flow-through, which contains the protein, was applied onto a Ni-NTA Superflow (Qiagen) column (2 × 2.5 cm) equilibrated with buffer A. The column was washed with 30 mL of buffer A and 50 mL of buffer A containing 1 M NaCl and then reequilibrated with buffer A, and the protein was eluted with 0.5 M imidazole in the above buffer. Ten milliliter fractions were collected and analyzed by Coomassie-stained SDS−PAGE gels. The protein-containing fractions were pooled and concentrated 20 times using a Ultrafree filter (Millipore) with a MW cutoff of 5000 Da. Imidazole was removed by several cycles of dilution−concentration with buffer A. The concentration of the sample was estimated by UV−visible spectroscopy using a calculated extinction coefficient of 2800 $M^{-1}\cdot cm^{-1}$ at 280 nm.

His-Tag Cleavage and Purification of ProS. The protein was digested at 25 °C in the presence of 2 mM $CaCl_2$ with 10 units of thrombin/mg of protein. The cleavage was complete after 1 h, and the protein was purified by gel filtration on a Sephadex HR-100 (Amersham Pharmacia Biotech) column (100 × 1.6 cm) equilibrated with buffer B (50 mM sodium phosphate, 50 mM NaCl, pH 7.0). One milliliter fractions were collected at a flow rate of 0.6 mL/min. The protein was eluted as a single peak, and the corresponding fractions were pooled and concentrated. About 10−12 mg of purified ProS were obtained from 20 g wet weight cells. Its purity was monitored by Coomassie-stained SDS−PAGE, ^{1}H NMR, and mass spectrometry.

Overexpression of ^{15}N-Labeled ProS. Uniformly ^{15}N-labeled ProS was overexpressed in 4 L of M9 minimal media supplemented with [^{15}N]ammonium chloride as sole nitrogen source and glucose. The ^{15}N-labeled ProS was purified according to the protocol described above.

Overexpression of ProS-PG-3 in Insect Cells. Recombinant baculovirus pPG3 allowing expression of pre-proprotegrin-3 and secretion in the culture medium of ProS-PG-3 was previously described (*8*). *Spodoptera frugiperda* (Sf9) cell cultures and virus productions were performed essentially as reported (*28*). *Trichoplusia ni* (High Five) cells were cultivated under similar conditions. Small-scale experiments have shown that the ProS-PG-3 production was substantially higher with High Five cells growing first for 24 h in serum-

supplemented medium TC100 and then for 48 h in serum-free medium when compared to production in Sf9 cells or High Five cells growing 48 or 72 h in serum-free medium. For infection, cells were plated at a density of 3×10^7 cells/175 cm^2 flask. One hour later, cells were infected with viral stocks at a multiplicity of infection (moi) ranging between 3 and 5. After removal of cell debris by centrifugation, culture medium was saved 72 h after infection and stored at −20 °C until processing.

Purification of ProS-PG-3. The proteins in the insect cell culture medium were ammonium sulfate precipitated (65% w/w). Then, in batches of about 30 mg of concentrated proteins, a first reverse-phase HPLC separation was performed on a C18 Oligo R3 POROS 40 × 300 mm preparative column (Perkin-Elmer, Les Ulis, France) with an acetonitrile gradient with 0.1% trifluoroacetic acid (10 mL/min). ProS-PG-3-containing fractions (50 mL) were identified by Western blot, pooled, concentrated by lyophilization, and subjected to a second HPLC separation on the same column with a slower gradient. Immunoreactive fractions were again pooled and concentrated by lyophilization. From 1.4 L of recombinant baculovirus-infected High Five cell culture medium, 15 mg of ProS-PG-3 was purified. The ProS-PG-3 purity was confirmed by Coomassie-stained SDS−PAGE, ^{1}H NMR, and mass spectrometry.

Building of a Model of the ProS Structure. Cathelicidins display a limited sequence homology with some cystatins. However, using the 3D-pssm program (http://www.bmm.icnet.uk/∼3dpssm/) a significant structural profile homology was identified between the prosequence of the porcine precursor protegrin-1 (Swiss-Prot number P32194) and the structure of the chicken cystatin (Swiss-Prot number P01038, PDB entry 1CEW). The two proteins were first aligned using the MULTIALIN software (*29*), and this alignment was then refined using the TITO program (*30*), which evaluated the compatibility of the aligned sequences with the chicken cystatin 3D structure. The 3D structure compatibility between ProS and the other cystatin structures (PDB entries 1A67 and 1A90) showed a lower score. Protein modeling was performed with the MODELLER program (*31*), and then the model was energy minimized by using the Discover package (Molecular Simulation Inc., San Diego, CA).

Mass Spectroscopy. The overexpressed ProS and ProS-PG-3 proteins were analyzed by the electrospray mass spectrometry technique (ES-MS) on a VG Bio-Q quadrupole with a mass range of 4000 Da (Bio-Tech, Manchester, U.K.) in positive mode. The proteins were desalted on Zip-Tip (Millipore), and 10 pmol was used for mass analysis. Scanning was performed from $m/z = 500$ Da to $m/z = 1700$ Da in 10 s. Calibration was performed using the multiply charged ions produced by a separate introduction of horse heart myoglobin (16 951.4 Da).

Circular Dichroism. CD spectra were recorded at room temperature on a CD6 Jobin-Yvon spectrophotometer. Spectra of ProS and ProS-PG-3 were measured at pH 3.0 using a 1 mm path-length cell on 200 μL of a 2.4×10^{-5} M solution. Each spectrum resulted from averaging five successive individual scans over the 195−250 nm wavelength range.

NMR. Spectra were referenced to TSP-d_4 as an external reference set at 0 ppm. The pH values were measured at room temperature with a 3 mm electrode. The pH was adjusted by the addition of 0.1 N HCl or 0.1 N NaOH. Freeze-dried ProS or ProS-PG-3 was dissolved in 0.45 mL of water ($H_2O/^2H_2O$, 95/5) giving a 1.3−1.4 mM solution.

All NMR experiments were performed on a Bruker AMX600 spectrometer, operating at 600 MHz and recorded by using a triple resonance probe. In all experiments, the carrier frequency was set at the center of the spectrum at the water frequency. Most of the spectra were recorded at 37 °C. DQF-COSY (*32*), z-TOCSY (*33*), and NOESY (*34*) spectra were acquired in the phase-sensitive mode using the States−TPPI method (*35*). Except for the DQF-COSY spectra (where low-power irradiation was used), the water resonance was suppressed by the WATERGATE method (*36*). z-TOCSY spectra were obtained with a mixing time of 80 ms and NOESY spectra with a mixing time of 150 ms.

For the uniformly ^{15}N-labeled ProS, ^{1}H−^{15}N HSQC experiments (*37*) were recorded with a 1.3 mM sample at pH 7.0 and at pH 3.0. All HSQC were recorded using a time domain data size of 256 t_1 × 1024 t_2 complex points and 32 transients per complex t_1 increments. ^{1}H−^{1}H−^{15}N TOCSY−HSQC (*38*) and NOESY−HSQC (*39*) 3D experiments were recorded with pulse sequences using gradient selections and with 400, 128, and 1024 complex points for the t_1, t_2, and t_3 time domains, respectively.

Data were processed by using either the XWIN-NMR or the GIFA (*40*) software. The data were zero-filled before processing, and shifted sine-bell functions were used for apodization. The processed data were baseline corrected using a five order polynomial function. The identification of the spin systems of ProS was obtained by analysis and comparison of COSY, TOCSY, and NOESY spectra. The sequential assignment was performed by using the general strategy described by Wüthrich (*41*).

RESULTS

Sequence Similarity Search and Secondary Structure Prediction. The primary sequence of ProS was analyzed for sequence similarity with proteins of the Swiss-Prot data bank and for secondary structure prediction. Results of PROSITE search (*42*) indicated that sequences spanning residues 34−47 and 78−100 are two cathelicidin signatures. The homology search with the MAXHOM program for multiple sequence alignment showed that 30 sequences share a sequence identity higher than 27% (Figure 1) (*43*). Sequences with a percentage of identity under 27% were discarded. The results of a secondary structure prediction obtained with the PHDsec program (*44*) indicated that the N-terminal part spanning residues 36−45/54 could adopt a helical structure, while sequences spanning 77−83 and 105−113 residues could adopt an extended structure (Figure 1). Most of the remaining parts of the sequence (mainly 61−76 and 86−94) are predicted as loops.

Building of a 3D Structure Model for ProS from the Chicken Cystatin Structure. Despite their low sequence similarity with cystatins (<25%), cathelicidins were classified in the cystatin superfamily. Depending on the details of alignment, ProS (101 residues) displays 20−22% of sequence similarity with that of the chicken cystatin (108 residues) (Figure 2). The cystatin structure was determined both by X-ray with a 2.0 Å resolution (PDB entry 1CEW) (*19*) and by NMR (PDB entry 1A67) (*20*−*22*). Although the two structures display a global fold consisting of an N-terminal helix cradled by a β-sheet of four antiparallel β-strands, they

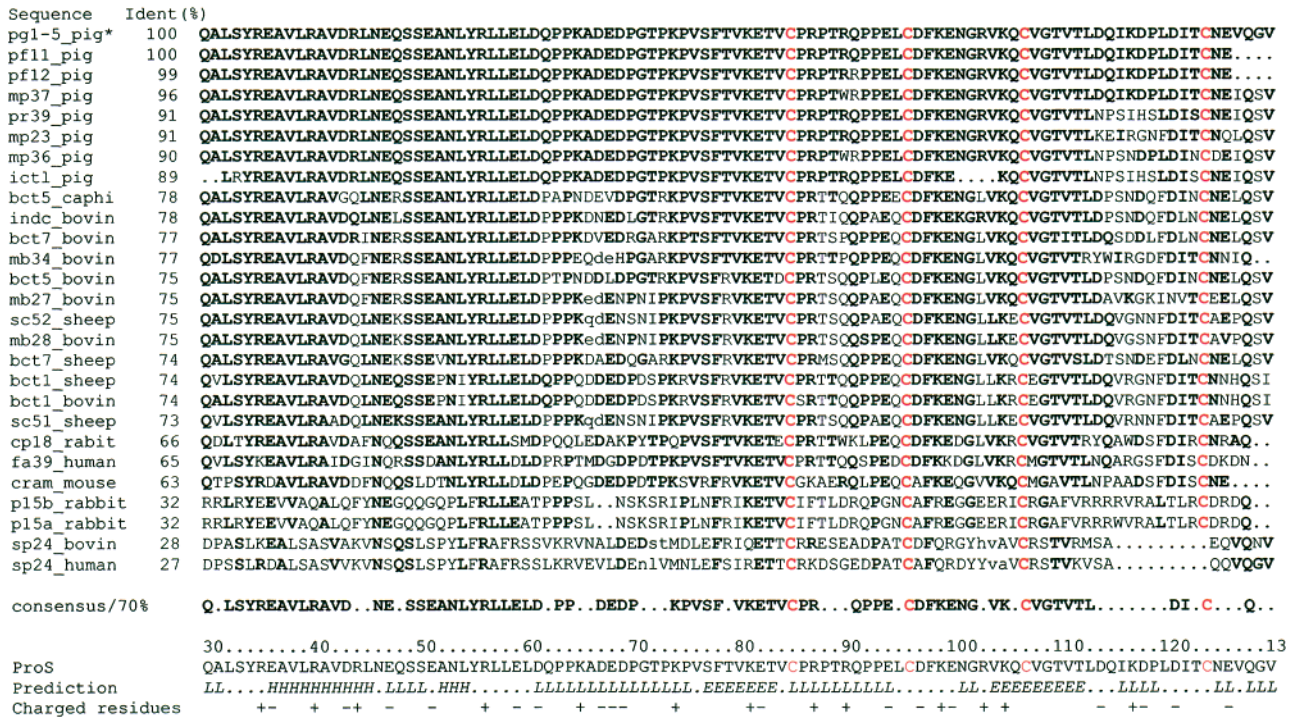

FIGURE 1: Sequence similarity search and secondary structure prediction for ProS. (Upper part) Sequence similarity search obtained by using the Protein Predict package program. Notice the conservation of the cysteine residues displayed in red (except for the sp24 sequences). Identical residues are displayed in bold. (Lower part) *L*, *H*, and *E* are for sequences predicted as loops, helix, and extended structures, respectively. The positively and negatively charged residues are identified all along the sequence by + and −, respectively. Abbreviations: pg1, pg2, pg3, pg4, and pg5 are for protegrin-1, -2, -3, -4, and -5 precursors, respectively; pf11 and pf12 are for prophenin-1 and -2 precursors, respectively; mp23, mp36, and mp37 are for pmap-23, pmap-36, and pmap-37 antibacterial peptide precursors, respectively; pr39_pig is for the antibacterial protein pr-39 precursor; ictl_pig is for cathelin; bct5 and bct7 are for bactenecin-5 and -7 precursors, respectively; bct1 is for the cyclic dodecapeptide precursor; indc bovin is for the indolicidin precursor; mb27, mb28, and mb34_bovin are for antibacterial peptides bmap-27, bmap-28, and bmap-34; sc51 and sc52 are for cathelin-related peptides; cp18 is for the antimicrobial protein cap18 precursor; fa39_human is for the antibacterial protein fall-39 precursor; cram_mouse is for the cathelin-related antimicrobial peptide precursor; p15a and p15b_rabbit are for 15 kDa protein a and b precursors; sp24 is for the secreted phosphoprotein 24 precursor. *, the prosequences for PG-1, PG-2, PG-3, PG-4, and PG-5 are identical.

significantly differ. Indeed, the 77−85 helix observed in the X-ray structure, which is not observed in the NMR structure, was hypothesized to be due to the crystal packing, whereby the segment 73−91 could adopt a different conformation (*20*). ProS and the chicken cystatin sequences have roughly the same size and contain two conserved disulfide bridges (see Discussion). A ProS model was built on the basis of the 3D structure of the chicken cystatin by using the MODELLER program. Two models of ProS were independently built from the NMR and the X-ray structures, and their quality was evaluated by the TITO program (*30*). The ProS model obtained from the crystal structure better satisfied the Cβ−Cβ distances than the model obtained from the NMR structure. The model of the ProS is displayed in Figure 2 by using the Molscript program (*45*).

Overexpression of ProS and ProS-PG-3. ProS, which contains two disulfide bonds, and ProS-PG-3, which contains four disulfide bonds, were overexpressed in the *E. coli* and in High Five insect cells, respectively.

ProS was overexpressed as a His-tagged protein and purified on a nickel column. After the thrombin cleavage, ProS contains four additional amino acids in its N-terminus, namely, G^{26}-S^{27} for the thrombin cleavage site and H^{28}-M^{29} which were generated by subcloning into the *Nde*I/*Bam*HI sites of the pET-15b. The ProS protein was characterized by Coomassie-stained SDS/PAGE, mass spectroscopy (MW = 11718.8 ± 0.3 Da, theoretical MW = 11718.3 Da), and NMR. Analytical gels of ProS at the different steps of overexpression and purification as well as its ES-MS spectrum are shown in Figure 3A. By using the same strategy, the uniformly ^{15}N-labeled ProS was obtained.

ProS-PG-3 (Q^{30}−G^{149}, 120 residues) was overexpressed in recombinant baculovirus-infected insect cells (High Five) and purified to homogeneity by RP-HPLC in two steps. The molecular mass of the protein which had an N-terminal glutamine-to-pyroglutamate modification and a C-terminal glycine instead of an amide group (MW = 13385.8 ± 0.5 Da) is in agreement with the expected mass (MW = 13385 Da) (*8*, *18*). Figure 3B displays the analytical gels corresponding to the overexpression and the purification of ProS-PG-3 as well as its mass spectrum.

CD Study. CD spectra of ProS and ProS-PG-3 presented in Figure 4 are very similar and are characterized by a minimum at 204−205 nm and a shoulder in the 222−225 nm range, indicating the presence of β-sheet and of α-helical structures, respectively. They are indicative of a similar global fold for the two proteins. Spectral analysis revealed that ProS and ProS-PG-3 structures mainly consist of β-strand (40−45%) and contain about 10−15% of α-helix.

NMR Measurements of ProS. The ProS ^{1}H NMR spectrum recorded at pH 7.0 showed a spreading of amide, αH, and side chain signals into characteristic ranges typically seen in proteins. Amide and αH signals were found in the 9.4−7.2 and 5.9−3.1 ppm ranges, respectively. Four well-

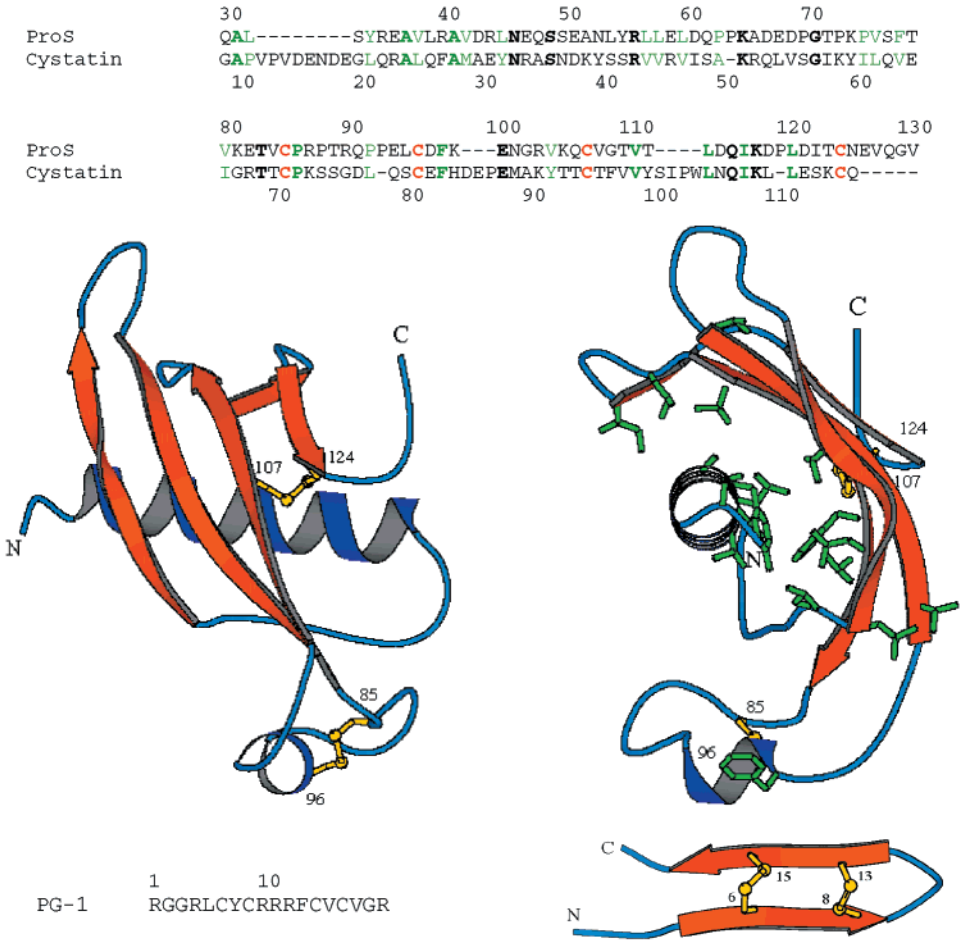

FIGURE 2: Sequence alignment and the ProS model built from the X-ray structure of the chicken cystatin (PDB entry 1CEW). (Upper panel) In the sequence alignment of ProS with the chicken cystatin (20% of identity), notice the alignment of the four cysteines in red. Identical residues are displayed in bold, and conserved hydrophobic residues in ProS and cystatin sequences are in green. Notice that for ProS and for the cystatin, their own numbering was used. (Middle panel) Two views of the model for the ProS structure, 90° apart. In the right view, the conserved hydrophobic residues in the ProS are displayed in green sticks. They are essentially located in the core of the molecule which consists of the interface area between the N-terminal helix and the wrapping β-sheet (see Discussion). (Lower panel) Sequence and schematic diagram of the antibacterial peptide PG-1 (*2*). The figure was drawn with the Molscript program (*45*). The disulfide bonds are displayed in yellow.

separated methyl signals of unequal intensity were observed at 0.52, 0.48, 0.42, and −0.05 ppm (Figure 5A). Clearly, the intensity of the signals at 0.42 and −0.05 ppm corresponds to one methyl group. Consequently, the two others weakly separated (0.52 and 0.48 ppm) did not individually integrate for one methyl group. Interestingly, these two signals in the 55/45 ratio together account for one methyl group, suggesting either the presence of two isoforms, two conformers, or an incomplete formation of the two disulfide bonds. The presence of the two isoforms was discarded by MS. In preliminary results, spectral alterations were observed in the presence of large amounts of the GSH/GSSG, 1/10, oxidative reagent (*46*). Therefore, data were incorrectly interpreted on the basis of the poor stability of one disulfide bond. We demonstrate here that, in the absence of the GSH/GSSG oxidative reagent, the intensities of the two sets of NMR signals were pH-modulated (see below), belong to two conformers, and are not due to the incomplete formation of disulfide bonds. Moreover, we established that the split methyl signals corresponded to the γCH_3 of V^{38}. The signal of the $\gamma' CH_3$ is the signal at −0.05 ppm.

The fingerprint area of the COSY experiment recorded at pH 7.0 showed more HN−C_αH cross-peaks than expected, and clearly, most of them were duplicated (data not shown). Similarly, the $^1H-^{15}N$ HSQC experiment also revealed more cross-peaks than expected. Most of them were split up in two neighboring signals of approximately the same intensity, suggesting that the two conformers roughly displayed the same basic 3D structure (Figure 5B).

A set of ProS ^1H NMR spectra was recorded as a function of pH from pH 7.0 to pH 3.0 (Figure 5A). These spectra show the gradual alterations of the methyl and αH signals induced by the progressive acidification. Clearly, the 0.52 ppm signal of the V^{38} γCH_3 became the major one at acidic pH and accounted for around 90% at pH 3.0. The methyl signal of the minor conformer was still observed at 0.48 ppm. Control experiments showed that these spectral alterations induced by acidification were reversible when the pH was increased to the neutral value. The $^1H-^{15}N$ HSQC experiment recorded at pH 3.0 shows the cross-peaks of the main conformers (Figure 5C).

Identification of the Conformational Exchange. Several indications, such as the intensity or alteration of the ratio of the V^{38} methyl signals by pH (see Discussion), suggested that the signal pairs observed in both COSY and HSQC experiments were due to the presence of two conformers for

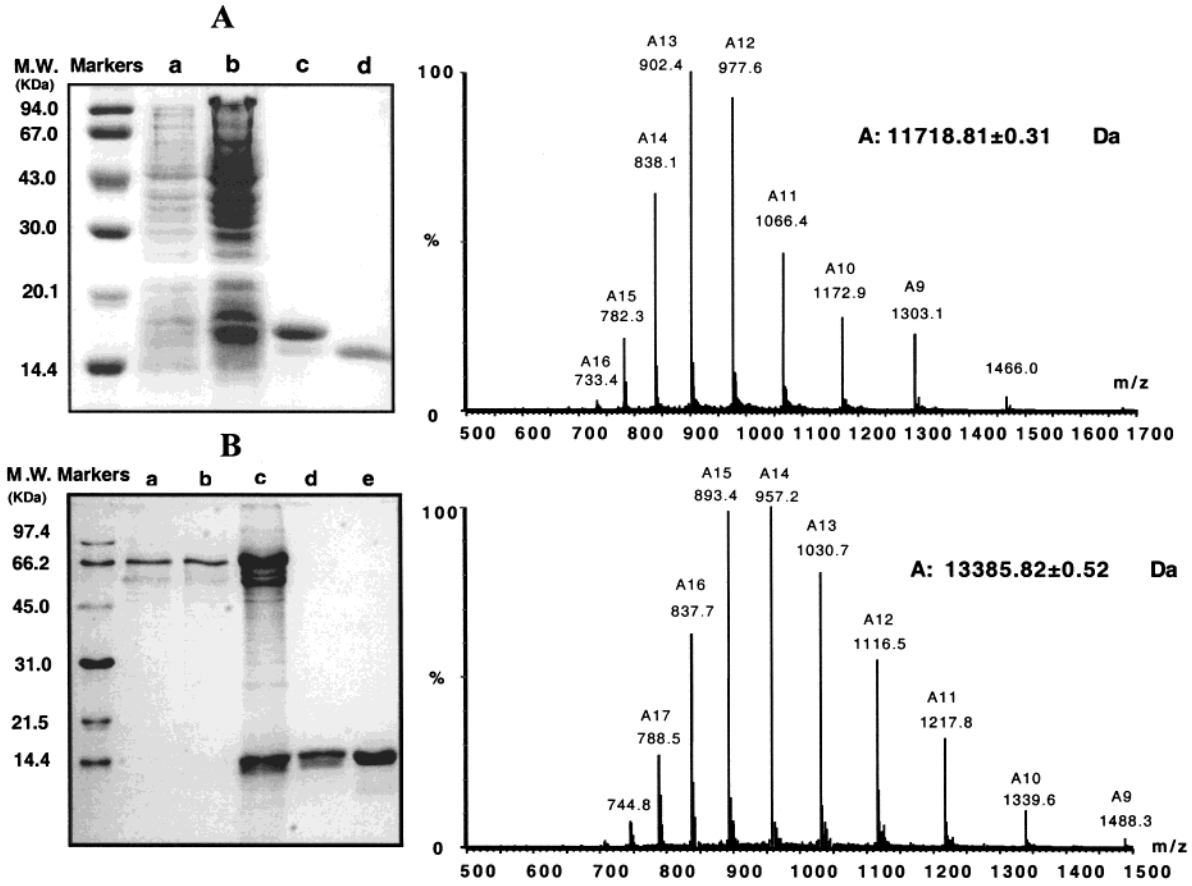

FIGURE 3: Coomassie-stained SDS−PAGE of (A) ProS and (B) ProS-PG-3 proteins overexpressed in *E. coli* and in High Five insect cells, respectively, at the different steps of their overexpression and purification. (A) Crude bacterial lysate before (lane a) and after IPTG induction (lane b), purified His-tagged protein (lane c), and the ProS protein after thrombin cleavage (lane d). (B) Medium from noninfected insect cells (lane a), medium of baculovirus-infected insect cells (lane b), concentrated medium of baculovirus-infected insect cells (lane c), and ProS-PG-3 after the first and the second HPLC purification (lanes d and e), respectively. The electrospray mass spectra of ProS and ProS-PG-3 are displayed on the right.

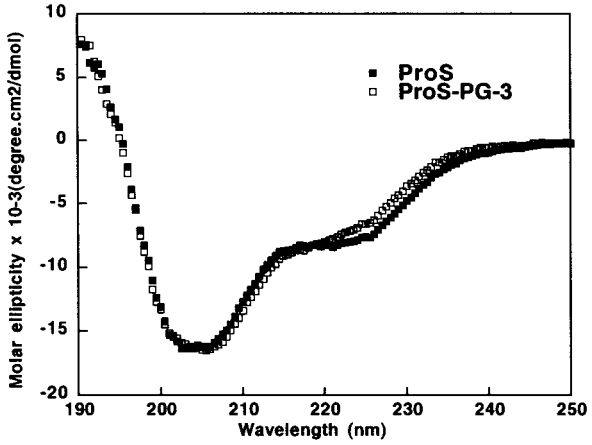

FIGURE 4: CD spectra of ProS and ProS-PG-3 recorded in water at pH 3.0.

ProS. Moreover, the simultaneous observation of their signals at 37 °C was indicative that they are in slow exchange on the ^{1}H chemical shift time scale. Unfortunately, in the NOESY experiment exchange and NOE cross-peaks have the same sign and therefore are difficult to distinguish. Usually, the ROESY experiment allows their identification. Here, we used the TOCSY experiment, which in this case appeared to detect exchange cross-peaks more sensitively. Indeed, in the TOCSY experiment the amide area is devoid of cross-peaks in the absence of exchange. In contrast, the observation of positive amide−amide cross-peaks in this area means that they are due to conformational exchange. Such cross-peaks were observed at 47 °C (Figure 6) whereas, due to a too low exchange rate, they were not observed at 37 °C (data not shown). Comparison with the NOESY spectrum allowed us to distinguish NOE and exchange cross-peaks (Figure 6). The observation of exchange cross-peaks strongly supported the slow exchange on the ^{1}H chemical shift time scale between the two conformers of ProS suggested by the signal pairs observed.

ProS and ProS-PG-3 Structural Data. (A) ProS. At neutral pH, due to the presence of two almost equally populated conformers, it appeared difficult to carry out the NMR structural study of ProS. Accordingly, we recorded a 2D NMR data set (COSY, TOCSY, NOESY) at pH 3.0 with the ≈90/10 mixture of conformers. Two parts of the ProS NOESY spectrum, recorded at 37 °C, are displayed in Figure 7. The assignment of fragments G^{26}−Q^{62}, K^{74}−P^{86}, E^{94}−I^{116} and L^{120}−V^{130} was obtained and accounts for about 80% of the sequence. In contrast, due to their high content in proline residues, the strong overlap of their spin systems, and the presence of the minor conformer, the assignment of the three remaining fragments, P^{63}−P^{73} (four prolines), R^{87}−P^{93} (three prolines), and K^{117}−P^{119} (one proline), was not achieved.

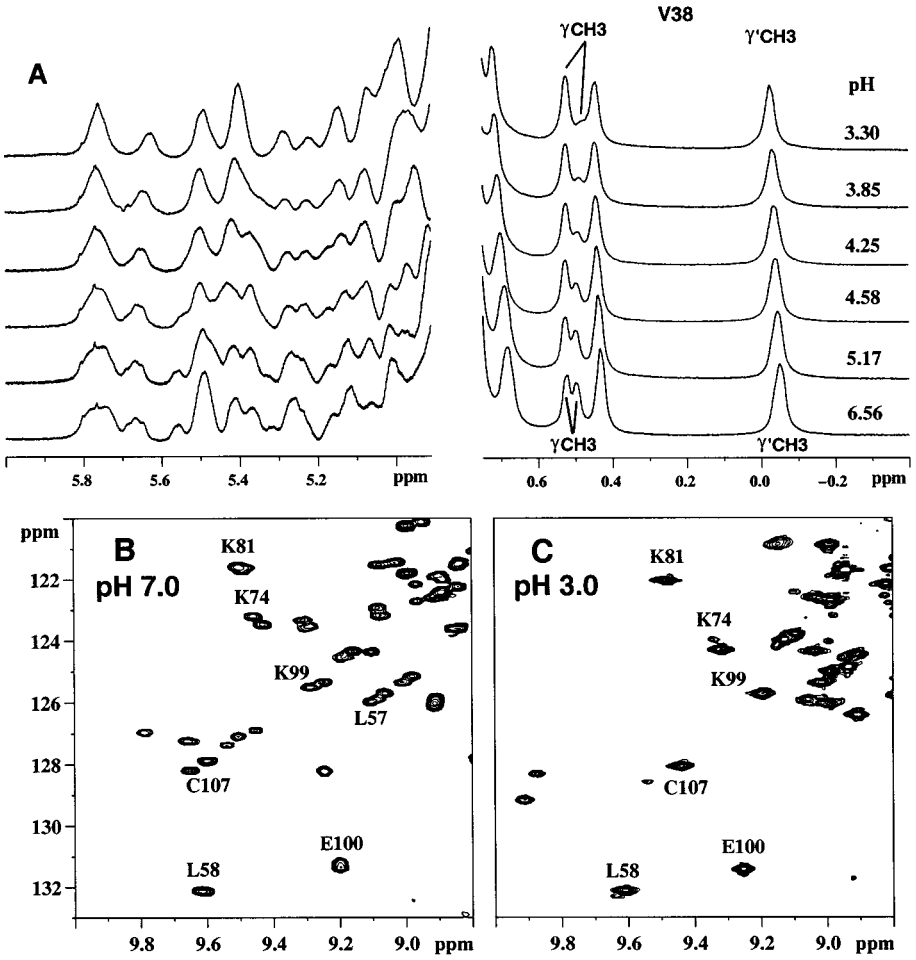

FIGURE 5: ^{1}H and $^{1}H-^{15}N$ HSQC spectra of ProS recorded as a function of pH at 37 °C. (A) Alterations of the αH (left) and methyl (right) signals of the ^{1}H NMR spectrum of ProS recorded as a function of pH. The progressive acidification converts the 55/45 split signal of the V^{38} γCH_3 (pH 6.56) to a major signal (pH 3.0). The two lines show the V^{38} γCH_3 signals for the two conformers of ProS. (B, C) Selected part of the $^{1}H-^{15}N$ HSQC spectra recorded at pH 7.0 and at pH 3.0, respectively. Several equally populated pairs of cross-peaks observed at neutral pH were converted into a major and a minor cross-peak at lower pH. Some of them are labeled. The map recorded at pH 3.0 shows cross-peaks of the main conformation of ProS.

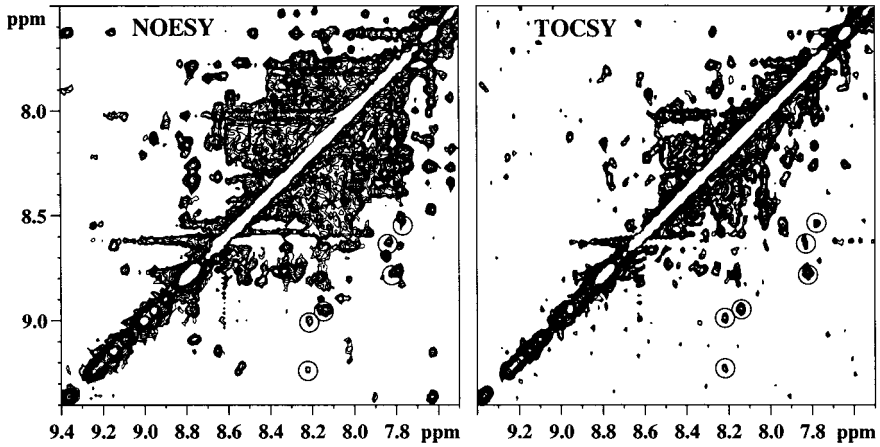

FIGURE 6: Amide−amide parts of the NOESY and TOCSY experiments of ProS recorded at 47 °C and pH 3.0. The NOESY map shows cross-peaks due to both NOE and exchange between conformers. The positive amide−amide cross-peaks of the TOCSY are due to the conformational exchange between the major and the minor conformers of the ProS. Several of these exchange cross-peaks are circled in the two maps.

(B) ProS-PG-3. ProS-PG-3 spectra as a function of pH showed the presence of two conformers at neutral pH, which were converted into a major one at pH 3.0 as observed for ProS (data not shown). The ProS-PG-3 NOESY spectrum was recorded at pH 3.0 and is displayed in Figure 7.

DISCUSSION

The Cathelicidin Motif Is a Widespread Motif in Antibacterial Precursors. A similarity search with the ProS sequence (101 residues) showed that, among the 27 sequences display-

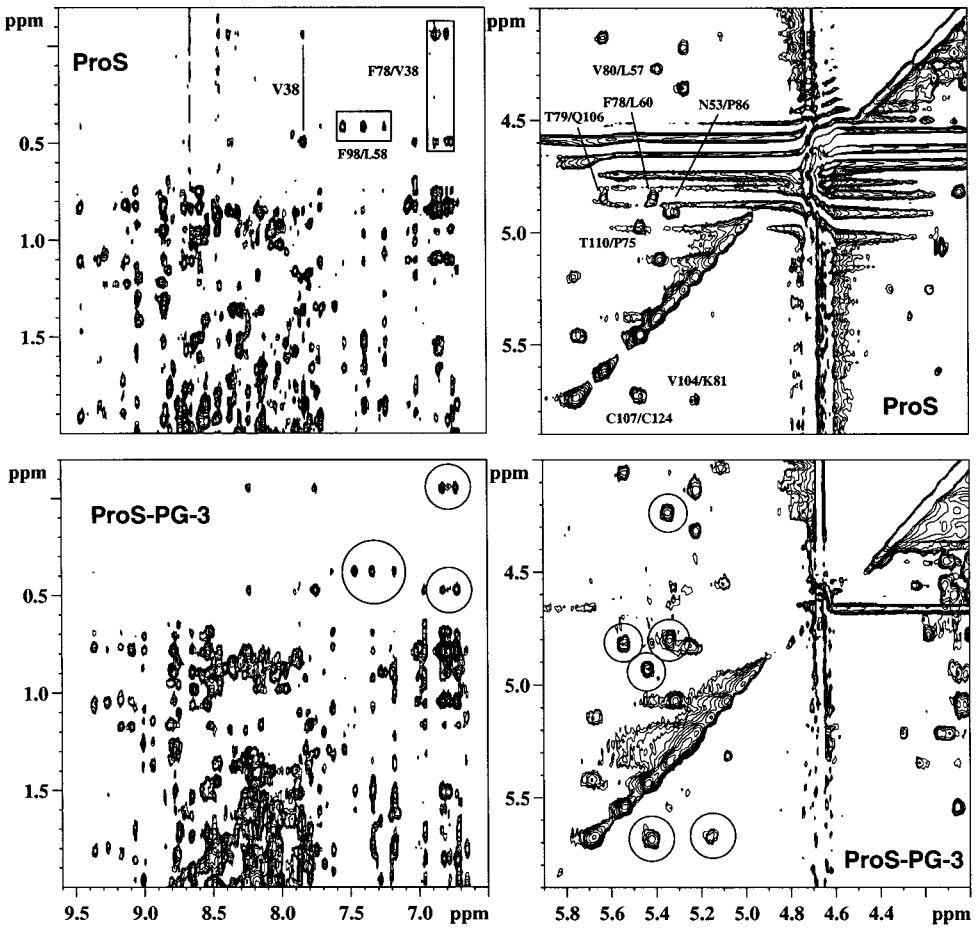

FIGURE 7: Two selected parts of the NOESY maps of ProS and ProS-PG-3 recorded at 37 °C and at pH 3.0 with a mixing time of 150 ms. For ProS, the V^{38} methyl signals, the F^{98}-L^{58} and F^{78}-V^{38} side chain NOEs (left part), and several $d_{\alpha\alpha}$ NOEs of the four-stranded β-sheet are labeled (right part). All of these key NOEs were observed and circled on the ProS-PG-3 spectra, suggesting a similar global fold for the two proteins which essentially differ by the protegrin sequence.

ing a sequence similarity higher than 27%, 25 are prosequences of antibacterial peptides whose mature C-terminal peptides belong to 15 different families. Most of these prosequences share a high similarity ranging from 63% to 99−100%, while three of them display a lower similarity ranging from 27% to 32%. Moreover, except for the sp24 sequences, the main feature of all these sequences is the conservation of the four cysteines, and potentially of the two disulfide bonds, as observed in the 70% consensus sequence (Figure 1). In addition, this consensus sequence shows the conservation of 7 out of the 10 prolines. Together, the high sequence similarity and the high conservation of cysteines and prolines, two structurally essential residues, suggested for these proteins a similar fold. These sequences mainly differ in their C-termini (17 residues), upstream of the various antibacterial sequences. Interestingly, all of these sequences show a high content in charged residues, (17 negatively and 13 positively charged residues for ProS), evenly spread along the sequence. Therefore, the excess of negatively charged side chains of the prosequence is consistent with the hypothesis of electrostatic interactions with the positively charged side chains of the antibacterial peptide. Nevertheless, due to the amphipathic character of PG, hydrophobic interactions should also to be taken into account. Such interactions could be responsible for the inactivation of the antibacterial peptide when it is still bound to its prosequence.

ProS and ProS-PG-3 Overexpression. To carry out a structural study of the cathelicidin motif of protegrin by NMR, both an efficient overexpression system and an easy strategy of purification were developed. ProS, which contains only two disulfide bonds and is devoid of the antibacterial sequence, was produced in *E. coli* as a His-tagged construct to facilitate its purification. Moreover, the main asset of this system is to allow the production of uniformly ^{15}N-labeled ProS suited for its NMR study.

In contrast, the baculovirus system in insect cells, known to possess the enzymatic machinery involved in the disulfide bond formation, was used to produce ProS-PG-3, which contains four disulfide bonds, two in the ProS sequence and two in the PG sequence. This expression system previously showed its ability to yield native-like ProS-PG-3 (*8*). Unfortunately, it is unsuited for the isotopic labeling.

Data Supporting the ProS Model. (A) The ProS Model. One feature of the cathelicidin family sequences is the presence of two disulfide bonds in the 1−2 and 3−4 pattern which has been demonstrated for the probactenecin and the prododecapeptide (*12*). Taking into account the high degree of sequence identity between the probactenecins and ProS (74−78%), the sequence location of the four cysteines, and the same length of the C^{85}−C^{96} and C^{107}−C^{124} spacing sequences, the disulfide bond arrangement of ProS and probactenecin was assumed to be identical (Figure 1). The C^{107}−C^{124} disulfide bond was confirmed by the $d_{\alpha\alpha}$ NOE

(Figure 7). DTT treatment of ProS dramatically altered its initial ^{1}H NMR spectrum, thus indicating the essential role of the two disulfide bonds in the maintainance of the 3D structure (data not shown).

Interestingly, ProS and cystatin sequences revealed a similar disulfide bond pattern. Moreover, a similar fold was proposed by the 3D-pssm server. Therefore, despite the low sequence similarity (20−22%), it was feasible to build a model on the basis of the X-ray cystatin structure. The global fold of the ProS model mainly consists of two helices spanning L^{32}−Q^{48} and P^{93}−D^{97} sequences and of four antiparallel β-strands (E^{59}−E^{68}, G^{71}−T^{83}, G^{102}−L^{113}, and L^{120}−C^{124}). In this model, helices and β-strands account for 22% and 42%, respectively.

(B) Identification of the Helix and of the Presence of β-Sheet in the Basic Fold of ProS. The CD spectrum revealed that the ProS and ProS-PG-3 structures consist mainly of β-strand and contain 10−15% of α-helix. One feature of the ProS and ProS-PG-3 ^{1}H NMR spectra is the presence of αH signals widely spread out from 5.9 to 3.1 ppm. According to the relationship between chemical shifts of αH protons and secondary structures, the highest and lowest chemical shift values are indicative of β-sheet and α-helix secondary structures, respectively (*47*−*50*).

On the basis of several successive d_{NN} NOEs, it clearly appeared that the N-terminal sequence spanning residues L^{32}−R^{44} adopted a helical structure whereas several long-range $d_{\alpha\alpha}$ NOEs (C^{107}−C^{124}, V^{104}−K^{81}, T^{110}−P^{75}, T^{79}−Q^{106}, F^{78}−L^{60}, N^{53}−P^{86} and V^{80}−L^{57}) allowed identification of four β-strands (N^{53}−L^{60}, P^{75}−P^{86}, V^{104}−T^{110} and I^{122}−E^{126}) giving rise to a β-sheet (Figure 7). Although incomplete, these NMR data indicated that the ProS structure consists of a well-defined helix located in the N-terminal part and of a four-stranded β-sheet, in good agreement with the proposed model built on the basis of the chicken cystatin structure (Figure 2).

(C) The Hydrophobic Core. Chicken cystatin and ProS sequences contain a similar percentage of hydrophobic residues (46% for cystatin and 44% for ProS). From the alignment proposed in Figure 2 it appeared that among the 45 hydrophobic residues of ProS, 26 (58%) are conserved. Interestingly, 18 of them (69%) are located in the inner sides of the helical part (A^{31}, Y^{34}, A^{37}, V^{38}, A^{41}, V^{42}, and L^{45}) and of the β-sheet (L^{57}, L^{60}, P^{63}, V^{76}, F^{78}, V^{80}, C^{107}, V^{111}, L^{113}, I^{116}, and C^{124}) (Figure 2). The interaction of these two secondary structures is supported by the NOE between the F^{78} and the V^{38} side chain located in the β-sheet and in the helix, respectively (Figure 7). All together, these hydrophobic residues give rise to a hydrophobic core which is, probably in part, responsible for the stability of the molecule. A similar hydrophobic cluster has been described for the oryzacystatin-I, a protein with no disulfide bonds, which displays the cystatin fold (*27*). The presence of such a hydrophobic core is supposed to contain "topohydrophobic" positions, known to be essential in the folding pathway and in the stability of globular structures (*51*, *52*).

ProS and ProS-PG-3 Structures Adopt Two Conformations. From the analysis of the V^{38} γCH_3 signals, the ratio of the two conformers (55/45 at neutral pH) was progressively and reversibly modified up to 90/10 by acidification. In contrast, the ratio remained unchanged for basic pH up to 10.4 (data not shown). This pH-mediated conformational change was also observed in the HSQC experiment as shown in Figure 5B,C. Moreover, since the chemical shifts of some residues are altered (C^{107}, K^{74}, K^{99}, L^{57}) and others are not or less (L^{58}, E^{100}, K^{81}), these data suggest that only one part of the molecule in involved in the conformational change. The presence of these two conformers is in agreement with the unique measured mass of 11 718.8 ± 0.3 Da, and the conformational exchange was clearly characterized at 47 °C. Such a pH-mediated conformational change suggests the involvement of some key electrostatic interactions between carboxylate groups (pK_a of Asp and Glu residues are in the 3−4 range) and side chains of positively charged residues. Notice that, for ProS-PG-3, a similar pH-mediated conformational change was observed. Moreover, the similarity of the CD (Figure 4) and their NOESY spectra (Figure 7) of ProS and ProS-PG-3 suggests a similar structure for the cathecidin part.

Interestingly, for the X-ray and solution structures of the chicken cystatin, the differences observed mainly involve the 73−91 sequence, a small "extra domain" which contains three glutamic (E^{82}, E^{86}, and E^{88}) and two aspartic (D^{77} and D^{85}) residues. Moreover, in the X-ray structure, the buried R^{43} side chain is oriented toward the short helix of the extra domain which contains a cluster of acidic residues (E^{82}, D^{85}, E^{86}) in such a way that electrostatic interactions could take place. On the contrary, in the solution structure, this 73−91 sequence is not structured, and the side chains of all of these acidic residues are solvated. These data support the propensity of this extra domain sequence to adopt different conformations, although they were not simultaneously observed (*20*). Interestingly, the sequence alignment shows that R^{43} and two acidic residues (E^{82} and E^{88}) of the cystatin are conserved in ProS as R^{56}, D^{97}, and E^{100}, respectively (Figure 2). Therefore, they are expected to be similarly located in the ProS model and involved in electrostatic interactions with the R^{56} side chain. The location of R^{56} in the core of the molecule in the neighbor of the V^{38} side chain would explain why the γCH_3 is able to monitor the conformational change induced by the involvement of the R^{56} side chain in electrostatic interactions, according to the ionization state of carboxyl groups. In contrast, the unchanged chemical shift measured for E^{100} makes unlikely its side chain involvement in such an interaction. Therefore, it appears reasonable to consider that the pH-mediated conformational change observed for ProS could be due to such intramolecular electrostatic interactions between the R^{56} side chain and acidic residues of the E^{82}−G^{102} extra domain sequence.

Location of the Protegrin in the ProS-PG-3 Structure with Regard to the Cystatin Fold. When compared to ProS, ProS-PG-3 data clearly indicated that neither the G^{26}SHM^{29} additional sequence at the N-terminus nor the presence of the highly constrained protegrin β-hairpin (Figure 2) was able to significantly modify the basic ProS structure. However, taking into account the model of the ProS structure and the protegrin structure which is particularly constrained, the location of its β-hairpin in the ProS-PG-3 structure can be speculated. Indeed, when linked to its prosequence, PG-3 can roughly adopt two positions with regard to ProS, one in which it is solvated as an extra domain and the other in which PG-3 is folded over and lies on the ProS structure. In this latter case the protegrin β-hairpin would enlarge the initial ProS β-sheet to give rise to a more globular structure with no or few alterations for the basic fold of the prosequence.

This would be consistent with the similar NMR data obtained for ProS and ProS-PG-3. We hope that the determination of the ProS-PG-3 structure, which is in progress, would allow us to experimentally demonstrate the location of PG with regard to its prosequence.

CONCLUSION

The determination of the 3D structure of the cathelicidin motif of the protegrin precursor, which is also widely encountered as the prosequence of other antibacterial peptides, should yield new insights into the interactions between ProS and PG responsible for the inactivation of its antibacterial activity. Moreover, this structural knowledge could be extended to the other antimicrobial precursors built on the same scheme. Such interactions could be further used in the design of small antibacterial peptides of therapeutic interest both to prevent potential toxicity and to improve their delivery to infected tissues.

ACKNOWLEDGMENT

We thank P. Mangeat for help in overexpression of ProS-PG-3, G. Labesse for help in the analysis of results from TITO, and C. Braud for the recording of CD spectra.

SUPPORTING INFORMATION AVAILABLE

Figure S1 showing slices of the NOESY-HSQC 3D experiment recorded at pH 3.0 showing the d_{NN} NOEs of the N-terminal part and Figures S2 and S3 showing the $^{1}H-^{15}N$ HSQC spectrum of ProS recorded at pH 7.0 (37 °C) and pH 3.0 (37 °C), respectively. This material is available free of charge via the Internet at http://pubs.acs.org.

REFERENCES

1. Kokryakov, V. N., Harwig, S. S., Panyutich, E. A., Shevchenko, A. A., Aleshina, G. M., Shamova, O. V., Korneva, H. A., and Lehrer, R. I. (1993) *FEBS Lett. 327*, 231−236.
2. Aumelas, A., Mangoni, M., Roumestand, C., Chiche, L., Despaux, E., Grassy, G., Calas, B., and Chavanieu, A. (1996) *Eur. J. Biochem. 237*, 575−583.
3. Fahrner, R. L., Dieckmann, T., Harwig, S. S., Lehrer, R. I., Eisenberg, D., and Feigon, J. (1996) *Chem. Biol. 3*, 543−550.
4. Suzuki, K., Shimoi, H., Iwasaki, Y., Kawahara, T., Matsuura, Y., and Nishikawa, Y. (1990) *EMBO J. 9*, 4259−4265.
5. Merkler, D. J. (1994) *Enzyme Microb. Technol. 16*, 450−456.
6. Zhao, C., Liaw, L., Lee, I. H., and Lehrer, R. I. (1997) *FEBS Lett. 410*, 490−492.
7. Shi, J., and Ganz, T. (1998) *Infect. Immun. 66*, 3611−3617.
8. Panyutich, A., Shi, J., Boutz, P. L., Zhao, C., and Ganz, T. (1997) *Infect. Immun. 65*, 978−985.
9. Valore, E. V., Martin, E., Harwig, S. S., and Ganz, T. (1996) *J. Clin. Invest. 97*, 1624−1629.
10. Zhao, C., Liu, L., and Lehrer, R. I. (1994) *FEBS Lett. 346*, 285−288.
11. Zanetti, M., Gennaro, R., and Romeo, D. (1995) *FEBS Lett. 374*, 1−5.
12. Storici, P., Tossi, A., Lenarcic, B., and Romeo, D. (1996) *Eur. J. Biochem. 238*, 769−776.
13. Scocchi, M., Wang, S., and Zanetti, M. (1997) *FEBS Lett. 417*, 311−315.
14. Wang, Y., Agerberth, B., and Johansson, J. (1998) *J. Protein Chem. 17*, 522−523.
15. Zanetti, M., Gennaro, R., Scocchi, M., and Skerlavaj, B. (2000) *Adv. Exp. Med. Biol. 479*, 203−218.
16. Gennaro, R., and Zanetti, M. (2000) *Biopolymers 55*, 31−49.
17. Gennaro, R., Scocchi, M., Merluzzi, L., and Zanetti, M. (1998) *Biochim. Biophys. Acta 1425*, 361−368.
18. Ritonja, A., Kopitar, M., Jerala, R., and Turk, V. (1989) *FEBS Lett. 255*, 211−214.
19. Bode, W., Engh, R., Musil, D., Thiele, U., Huber, R., Karshikov, A., Brzin, J., Kos, J., and Turk, V. (1988) *EMBO J. 7*, 2593−2599.
20. Engh, R. A., Dieckmann, T., Bode, W., Auerswald, E. A., Turk, V., Huber, R., and Oschkinat, H. (1993) *J. Mol. Biol. 234*, 1060−1069.
21. Dieckmann, T., Mitschang, L., Hofmann, M., Kos, J., Turk, V., Auerswald, E. A., Jaenicke, R., and Oschkinat, H. (1993) *J. Mol. Biol. 234*, 1048−1059.
22. Gerhartz, B., Engh, R. A., Mentele, R., Eckerskorn, C., Torquato, R., Wittmann, J., Kolb, H. J., Machleidt, W., Fritz, H., and Auerswald, E. A. (1997) *FEBS Lett. 412*, 551−558.
23. Janowski, R., Kozak, M., Jankowska, E., Grzonka, Z., Grubb, A., Abrahamson, M., and Jaskolski, M. (2001) *Nat. Struct. Biol. 8*, 316−320.
24. Martin, J. R., Craven, C. J., Jerala, R., Kroon-Zitko, L., Zerovnik, E., Turk, V., and Waltho, J. P. (1995) *J. Mol. Biol. 246*, 331−343.
25. Stubbs, M. T., Laber, B., Bode, W., Huber, R., Jerala, R., Lenarcic, B., and Turk, V. (1990) *EMBO J. 9*, 1939−1947.
26. Lee, S. Y., Lee, J. H., Chang, H. J., Cho, J. M., Jung, J. W., and Lee, W. (1999) *Biochemistry 38*, 2340−2346.
27. Nagata, K., Kudo, N., Abe, K., Arai, S., and Tanokura, M. (2000) *Biochemistry 39*, 14753−14760.
28. Andreoli, C., Martin, M., Le Borgne, R., Reggio, H., and Mangeat, P. (1994) *J. Cell Sci. 107*, 2509−2521.
29. Corpet, F. (1988) *Nucleic Acids Res. 16*, 10881−10890.
30. Labesse, G., and Mornon, J. (1998) *Bioinformatics 14*, 206−211.
31. Sali, A., and Blundell, T. L. (1993) *J. Mol. Biol. 234*, 779−815.
32. Rance, M., Sorensen, O. W., Bodenhausen, G., Wagner, G., Ernst, R. R., and Wuthrich, K. (1983) *Biochem. Biophys. Res. Commun. 117*, 479−485.
33. Rance, M. (1987) *J. Magn. Reson. 74*, 557−564.
34. Macura, S., Huang, Y., Sutter, D., and Ernst, R. R. (1981) *J. Magn. Reson. 43*, 259−281.
35. Marion, D., Ikura, M., Tschudin, R., and Bax, A. (1989) *J. Magn. Reson. 85*, 393−399.
36. Piotto, M., Saudek, V., and Sklenar, V. (1992) *J. Biomol. NMR 2*, 661−665.
37. Bax, A., Ikura, M., Kay, L. E., Torchia, D. A., and Tschudin, R. (1990) *J. Magn. Reson. 86*, 304−318.
38. Marion, D., Kay, L. E., Sparks, S., Torchia, D. A., and Bax, A. (1989) *J. Am. Chem. Soc. 111*, 1515−1517.
39. Marion, D., Driscoll, P. C., Kay, L. E., Wingfield, P. T., Bax, A., Gronenborn, A. M., and Clore, G. M. (1989) *Biochemistry 28*, 6150−6156.
40. Pons, J. L., Malliavin, T. E., and Delsuc, M. A. (1996) *J. Biomol. NMR 8*, 445−452.
41. Wüthrich, K. (1986) *NMR of Proteins and Nucleic Acids*, John Wiley & Sons, New York.
42. Hofmann, K., Bucher, P., Falquet, L., and Bairoch, A. (1999) *Nucleic Acids Res. 27*, 215−219.
43. Sander, C., and Schneider, R. (1991) *Proteins 9*, 56−68.
44. Rost, B., and Sander, C. (1993) *J. Mol. Biol. 232*, 584−599.
45. Kraulis, P. J. (1991) *J. Appl. Crystallogr. 24*, 946−950.
46. Sanchez, J. F., Wojcik, F., Strub, M. P., Chavanieu, A., Lehrer, R., Ganz, T., Calas, B., and Aumelas, A. (2001) in *Peptides 2000, Proceedings of the 26th European Peptide Symposium* (Martinez, J., and Ferhentz, J. A., Eds.) pp 525−526, EDK, Montpellier.
47. Lee, M. S., Palmer, A. G. d., and Wright, P. E. (1992) *J. Biomol. NMR 2*, 307−322.
48. Wishart, D. S., Bigam, C. G., Holm, A., Hodges, R. S., and Sykes, B. D. (1995) *J. Biomol. NMR 5*, 67−81.
49. Wishart, D. S., and Sykes, B. D. (1994) *Methods Enzymol. 239*, 363−392.
50. Wishart, D. S., Sykes, B. D., and Richards, F. M. (1991) *J. Mol. Biol. 222*, 311−333.
51. Poupon, A., and Mornon, J. P. (1998) *Proteins 33*, 329−342.
52. Reddy, B. V., Li, W. W., Shindyalov, I. N., and Bourne, P. E. (2001) *Proteins 42*, 148−163.

BI010930A